Society For Biomaterials

Osteoblast response to the surface topography of hydroxyapatite two-dimensional films

Gai Yang,[1] Zili Liu,[1] Yuming Guo,[1,2] Jie Zhang,[1] Han Li,[1] Weike Shi,[1] Jing Feng,[1] Kui Wang,[1] Lin Yang[1,2]

[1]Collaborative Innovation Center of Henan Province for Green Manufacturing of Fine Chemicals, Key Laboratory of Green Chemical Media and Reactions, Ministry of Education, Henan Normal University, Xinxiang, Henan 453007, People's Republic of China

[2]Henan Key Laboratory of Green Chemical Media and Reactions, School of Chemistry and Chemical Engineering, Henan Normal University, Xinxiang, Henan 453007, People's Republic of China

Received 30 August 2016; revised 2 November 2016; accepted 23 November 2016
Published online 23 January 2017 in Wiley Online Library (wileyonlinelibrary.com). DOI: 10.1002/jbm.a.35967

Abstract: In the current study, three hydroxyapatite two-dimensional films with similar wettability but different topological roughness have been prepared through a facile one-step method using hydrated polylactic acid discs as substrates. The results indicated that the protein adsorption capabilities of the hydroxyapatite two-dimensional films and the proliferation of osteoblast cells on the as-prepared films increased obviously with the increase of the films' roughness. These reveal that the cellular responses to two-dimensional materials can be efficiently tuned by easily adjusting the topological roughness. This finding affords an efficient strategy to regulate the cellular response to bioinorganic two-dimensional materials and significantly expanded their application potentials in tissue engineering. © 2017 Wiley Periodicals, Inc. J Biomed Mater Res Part A: 105A: 991–999, 2017.

Key Words: hydroxyapatite; two-dimensional films; roughness; osteoblast; cellular response

How to cite this article: Yang G, Liu Z, Guo Y, Zhang J, Li H, Shi W, Feng J, Wang K, Yang L. 2017. Osteoblast response to the surface topography of hydroxyapatite two-dimensional films. J Biomed Mater Res Part A 2017:105A:991–999.

INTRODUCTION

Recently, bioinorganic materials have exhibited promising applications in tissue engineering, such as metal oxide,[1–4] calcium phosphate,[5,6] and calcium carbonate,[7,8] in which the materials with excellent topographical properties that can elicit the specific cellular responses have attracted considerable attention.[9–15] From studies, the interactions between inorganic materials and human cells are critical for their practical applications in tissue engineering. Previous studies suggested that the interactions of inorganic materials with human cells highly depend on their specific surface properties, for example, roughness and surface wettability.[16–18] For example, aluminum oxide films with rough surface could promote the attachment and proliferation of human fibroblasts.[19] However, the aluminum oxide films with smooth surface could not exhibit this promotion effects. However, the studies about the qualitative or semi-quantitative dependence of the cellular response on the roughness of the inorganic materials are scarcely reported.

As one of the important research fields of tissue engineering, bone defects repair has attracted tremendous attention in recent years. As the disease with high incidence rate, bone defects pose the serious threat to human health.[20] Previous studies suggested that hydroxyapatite (HA) was an excellent material for bone defects repair and the current research about the bone defects repair focus on the biological effects of chemical composition and structure of nanoscaled building units of HA.[21,22] For example, carbonate content of carbonated HA could modulate the cellular behaviors of the osteoblasts.[23] With the increase of the carbonate content, the differentiation of the osteoblasts decreased. However, human bones are organic–inorganic nanoassemblies of HA nanocrystals and proteins. More importantly, human bones are not the smooth assemblies but exhibit exceptional surface topological structures that can affect the behaviors of the osteoblasts significantly.[24] Therefore, it is critical to study the effects of the surface topological properties of the two-dimensional films composed of nanoscaled building units of HA on the behaviors of the osteoblasts.

Herein, three HA two dimensional (2D) films with different roughness but similar wettability were prepared through

Correspondence to: Y. Guo; e-mail: guoyuming@htu.edu.cnor L. Yang; e-mail: yanglin1819@163.com
Contract grant sponsor: National Natural Science Foundation of China; contract grant numbers: 21171051, 21271066, U1204516
Contract grant sponsor: Program for Science & Technology Innovation Talents in Universities of Henan Province; contract grant number: 13HASTIT011
Contract grant sponsor: Key Young Teachers Project of Henan Province; contract grant number: 2012GGJS-065

a facile method. The effect of the roughness of the films on the osteoblast response was studied. The results indicated that the roughness of the films significantly influenced the protein adsorption capacity and the proliferation of the osteoblast. The lower the roughness, the higher the pro-proliferation activity. These suggest that the protein adsorption capacities and the corresponding cellular responses to 2D materials might be successfully regulated through the adjustment of the roughness. This affords a novel idea for the regulation of the cellular response to 2D materials and expanded their application potentials in tissue engineering.

MATERIALS AND METHODS

Preparation of hydrated polylactic acid discs

Round polylactic acid (PLA) discs with the diameter of 7.5 mm were ultrasonicated for 10 min in the mixture of hydrochloric acid and absolute ethanol with the volume ratio of 1: 3 and rinsed with double distilled water (DD water) to remove the grease on the surface. The clean PLA discs were incubated with 0.1 *M* NaOH aqueous solution at 25°C for 4 h, rinsed with DD water, and dried at room temperature to prepare hydrated PLA discs.

Preparation of HA 2D films

In the current study, hydrated PLA discs were used as substrates to prepare HA 2D films. From literature, using different amino acids as organic matrices, HA crystals with different crystallinity and morphology could be successfully prepared.[25,26] Therefore, three different HA 2D films were fabricated using three amino acids as organic matrices, including arginine (Arg), aspartic acid (Asp), and glycine (Gly), respectively. First, $CaCl_2$ aqueous solution (10 mL, 50 m*M*) was added slowly dropwise into amino acid aqueous solution (30 mL, 30 m*M*) and was stirred at 25°C for 2 h to allow the completely interaction between Ca^{2+} and amino acid. Then, $NaH_2PO_4{\cdot}2H_2O$ aqueous solution (10 mL, 30 m*M*) was added slowly dropwise into the mixed solution of $CaCl_2$ and amino acid. The pH value of the system was adjusted to 6.00. Subsequently, the hydrated PLA discs were placed onto the surface of the solution and was reacted at 25°C for 5 days. Finally, the as-prepared HA 2D films were collected and rinsed with DD water, dried under vacuum and denoted as HA/Arg/PLA, HA/Asp/PLA, and HA/Gly/PLA, respectively.

For comparison, the control experiment was performed using unhydrated PLA discs as substrate under nearly identical conditions as the typical experiment.

Characterization

The surface morphologies and roughness parameters of the HA 2D films were characterized by scanning electron microscopy (SEM, JSM-6390LV, JEOL) and atomic force microscopy (AFM, Bruker). The polymorphs of the 2D films were characterized by powder X-ray diffraction (XRD) using a D8 ADVANCE X-ray diffractometer (Bruker axs Com., Germany) with graphite monochromatized Cu Kα radiation ($\lambda = 0.15406$ nm) in the 2θ range of 20–70°. The wettability of the 2D films was evaluated using a contact angle (CA) goniometer (DSA25, KRUSS).

Cell culture

In this study, hFOB 1.19 human osteoblast cells (ATCC No. CRL-11372) were cultured in 1:1 mixture of Ham's F12 Medium Dulbecco's Modified Eagle's Medium supplemented with heat-inactivated FBS (10%), Penicillin (100 units/mL), Streptomycin (100 μg/mL), amphotericin B (fungizone, 0.25 μg/mL), G418 (0.3 mg/mL), L-glutamine (2.5 m*M*), and sodium bicarbonate (1.5 mg/mL) in a humidified incubator at fully humidified atmosphere at 34°C, 5% CO_2, and 95% room air.

Effect of HA 2D films on the proliferation of hFOB 1.19 cells

Culture media of 200 μL containing hFOB 1.19 cells with initial cell density of 2.5×10^4 cells/mL were pippetted onto the surface of the different HA 2D films separately placed in the wells of 96-well flat bottom culture microplates and incubated for 72 h in a humidified incubator at fully humidified atmosphere at 34°C, 5% CO_2, and 95% room air. The cultivation of the cells in the wells without HA 2D films under same conditions was denoted as the control. The proliferation of the cells was determined by MTT colorimetric assay. Briefly, after 72 h treatment, 20 μL of freshly prepared MTT (3–(4,5-dimethylthiazol-2-yl)-2,5,diphenyl tetrazolium bromide, 5 mg/mL in PBS) was added to each well and incubated at 37°C, under 5% CO_2 for 5 h. Then, the supernatant was carefully discarded and 150 μL of DMSO were added to each well to dissolve the dark blue crystals completely. The solution in each well was carefully transferred to well of another fresh culture microplate and the absorbance of the solution in each well at the wavelength 570 nm was determined by a microplate reader. The extent of cell proliferation was reflected by the average value of absorbance while the viability of the treatment by different HA 2D films were calculated by Eq. (1). The data were reported as mean ± standard deviation (SD) based on the measurements of the six samples.

$$\text{Viability } (\%) = \frac{O.D._{570\text{nm}} \text{ of treatment group}}{O.D._{570\text{nm}} \text{ of control group}} \times 100 \quad (1)$$

Determination of concentrations of adsorbed protein on HA 2D films

The concentrations of the absorbed proteins on HA 2D films were determined by bicinchoninic acid (BCA) assay. Briefly, 200 μL of culture media were pippetted onto different HA 2D films separately placed in the wells of 96-well flat bottom plates and incubated for 4 h at 37°C. Then, the films were transferred into 2.0 mL protein lobind tube (one film per tube) and rinsed twice with 600 μL of PBS buffer to remove the non-adherent proteins. Then, 240 μL of a 1 wt % aqueous solution of SDS were added and shaken for 1 h at room temperature to collect the protein adsorbed on the films' surface. This procedure was repeated twice and all

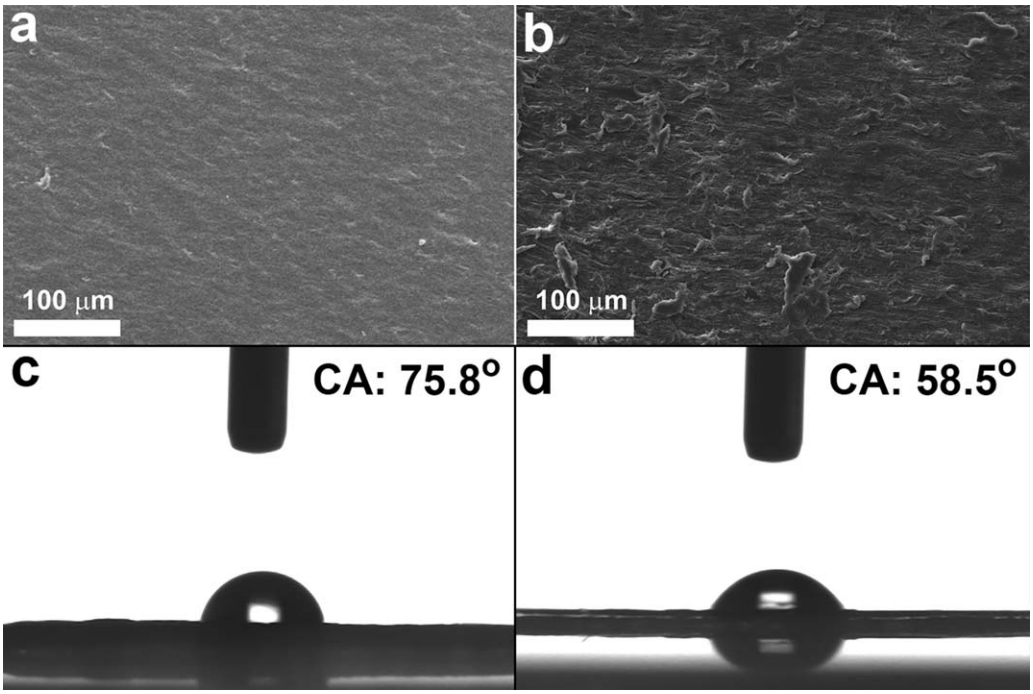

FIGURE 1. SEM images of (a) original unhydrated and (b) hydrated PLA discs. Optical images of the water contact angles measurement of (a) unhydrated and (b) hydrated PLA discs.

the SDS solution was collected in protein lobind tube. Subsequently, 125 μL of BCA working solution were added to each tube, gently mixed, incubated at 60°C for 15 min, and cooled to room temperature. Finally, the concentrations of protein in the collected SDS solutions were determined by measuring the absorbance at the wavelength 562 nm. Bovine serum albumin was used to prepare solutions in SDS with eight known concentrations to construct the standard curve.

RESULTS

Characterization of original unhydrated and hydrated PLA discs

The morphologies of the original unhydrated and hydrated PLA discs were determined by SEM. From the results shown in Figure 1(a,b), the original unhydrated PLA discs exhibit smooth surface. However, the hydrated PLA discs exhibit comparatively rough surface. In addition, from the water CA analysis results shown in Figure 1(c,d), the water CA of the hydrated PLA discs is 58.5°, significantly lower than that of the original unhydrated PLA discs (75.8°). These results indicate that the hydration pre-treatment can obviously enhance the roughness and wettability of the PLA discs.

Characterization of HA 2D films

The morphologies of the as-prepared HA 2D films were characterized by SEM. From SEM images shown in Figure 2(a,b), HA-Asp-PLA film is composed of nanoplates with the thickness of about 77 nm. From Figure 2(c,d), similar to HA-Asp-PLA films, HA-Arg-PLA film is also composed of nanoplates. However, the thickness of the nanoplates is about 100 nm, obviously thicker than that of the HA-Asp-PLA film. From Figure 2(e,f), HA-Gly-PLA film is composed of nanoribbons with the width of about 980 nm and thickness of about 70 nm. For comparison, it was attempted to prepare HA 2D films using unhydrated PLA discs as substrate under nearly identical conditions as the typical experiment. However, the result showed that HA 2D films could not be formed on unhydrated PLA discs (Fig. 3).

From XRD patterns shown in Figure 4, all the HA 2D films exhibit similar diffraction patterns, in which the diffraction peaks located at 25.9°, 31.7°, 39.8°, 46.7°, 49.5°, 53.2°, and 64.1° can be attributed to (002), (211), (130), (222), (213), (004), and (323) planes of the hexagonal HA phase (JCPDF 73–0293). No obvious diffraction peaks from other impurities are observed. These results clearly indicate the successful formation of HA.

The surface morphology and topological roughness of HA 2D films were characterized by AFM. From the results shown in Figure 5(a–c), three HA 2D films exhibited rough surface with different mean square roughness (RMS). The RMS roughness of HA-Asp-PLA, HA-Arg-PLA, and HA-Gly-PLA 2D films were determined as 756.6 nm, 859.5 nm, and 941.9 nm, respectively.

To evaluate the wettability of the HA 2D films, water CAs of the films were measured. From the results shown in Figure 5(d–f), water droplets can spread out well on the surfaces of the HA 2D films. The CAs of HA-Asp-PLA, HA-Arg-PLA, and HA-Gly-PLA 2D films were determined as 21.8°, 20.9°, and 22.5°, respectively, clearly indicating the similarly good hydrophilicity of the HA 2D films.

Osteoblast response to HA 2D films

In this study, the proliferation of the osteoblast cells on the as-prepared HA 2D films were studied by MTT assay, in

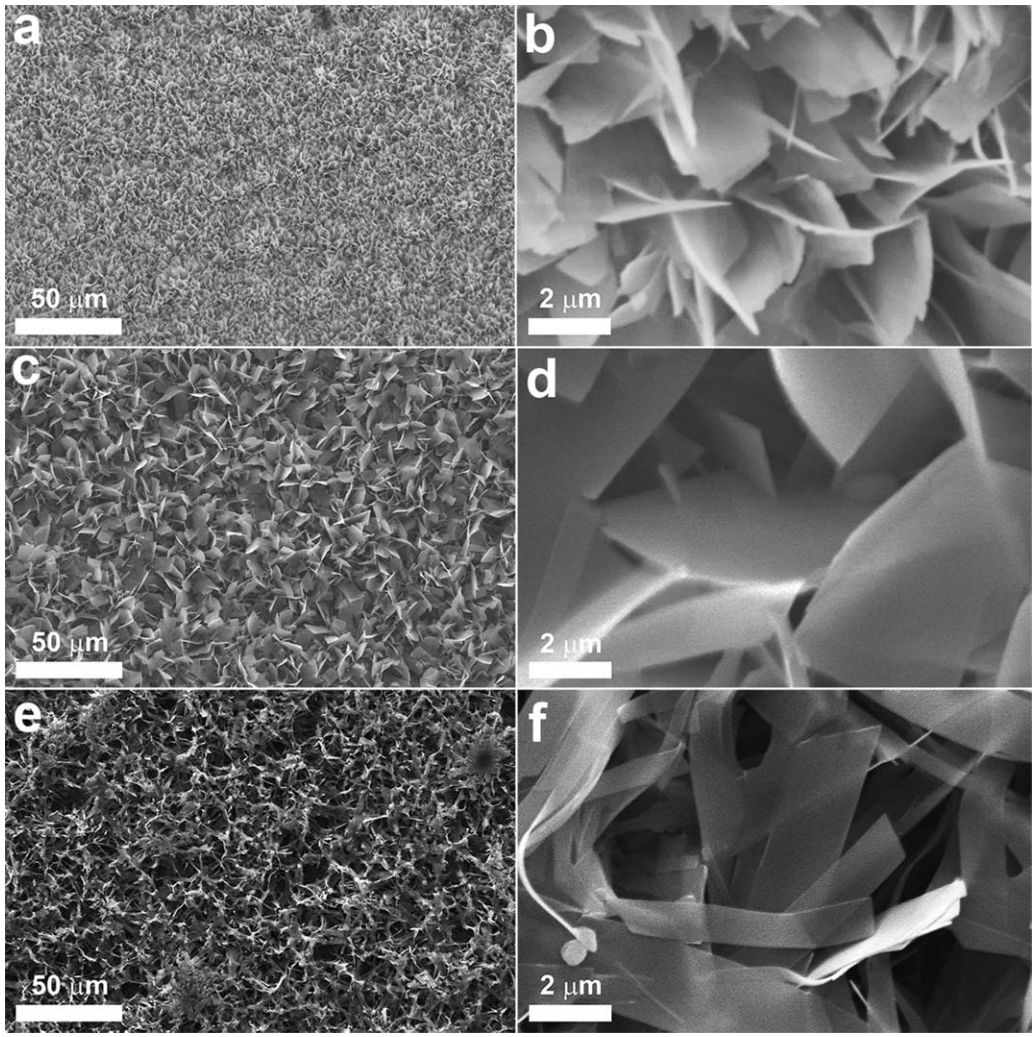

FIGURE 2. SEM images of (a,b) HA-Asp-PLA, (c,d) HA-Arg-PLA, and (e,f) HA-Gly-PLA 2D films.

which the viability of the cells cultivated in the control well was set as 100%. From Figure 6(a), the viabilities of the cells cultivated on HA-Asp-PLA, HA-Arg-PLA, and HA-Gly-PLA 2D films were determined as $123.7 \pm 1.5\%$, $153.3 \pm 2.7\%$, and $175.5 \pm 2.4\%$, respectively. Compared with the control group, the viabilities of the cells cultivated on three HA 2D films increased significantly. This indicates that the as-prepared HA 2D films can significantly promote the growth of the osteoblast cells. From optical micrographs shown in Figure 6(b–e), osteoblast cell densities cultured on HA 2D films are considerably higher than that on the control well, which directly confirmed the pro-proliferation activities of HA 2D films on osteoblast cells.

Furthermore, the promotion effects of the three films on proliferation of osteoblast cells are obviously different, in which HA-Gly-PLA 2D film with the biggest RMS exhibits

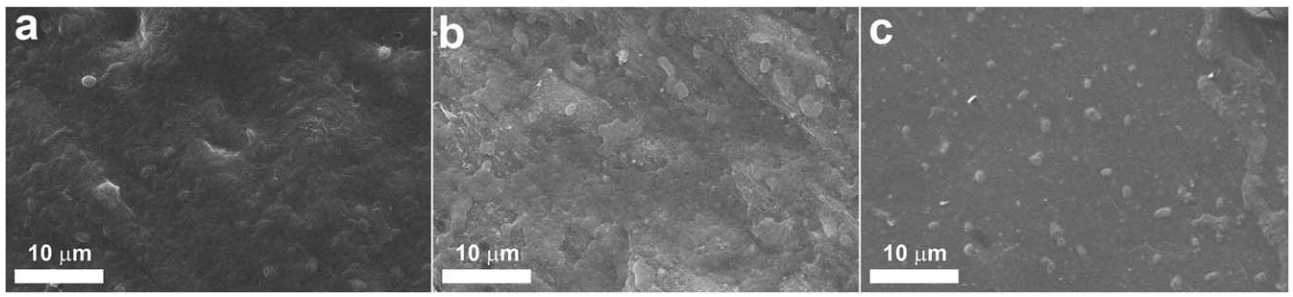

FIGURE 3. SEM images of the products prepared on unhydrated PLA discs using different amino acids as matrices under nearly identical conditions as the typical experiment. (a) Asp, (b) Arg, (c) Gly.

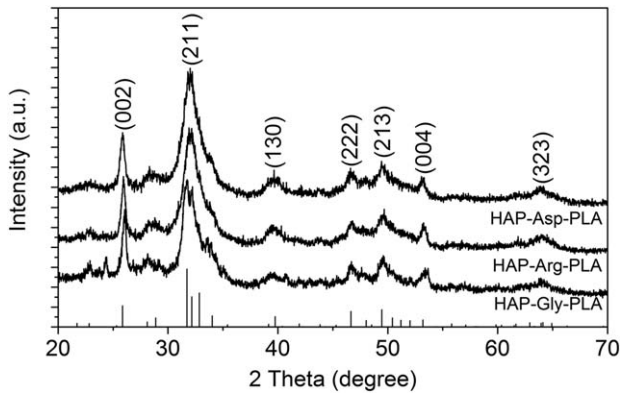

FIGURE 4. XRD patterns of HA-Asp-PLA, HA-Arg-PLA, and HA-Gly-PLA 2D films.

the strongest promotion effect on the proliferation of osteoblast cells. In comparison, HA-Asp-PLA 2D film with the smallest RMS exhibits the weakest promotion effect. Because of the same chemical compositions and similar wettability, the different pro-proliferation activities of HA 2D films might be attributed to their different topological roughness.

In addition, using HA-Arg-PLA 2D film as an example, the hFOB 1.19 cells cultured on HA 2D films were observed by SEM. From the results shown in Figure 7, similar to the hFOB 1.19 cells cultured on control wells shown in Figure 7(a,b), the hFOB 1.19 cells can also attach well onto the HA-Arg-PLA 2D film and exhibit the identical morphology with that of the control [Fig. 7(c,d)]. Moreover, the hFOB 1.19 cells cultured on HA-Arg-PLA 2D appear much flatter and spreading out better than those on control wells.

According to previous studies, the capacities of the surfaces to adsorb proteins from culture medium may influence the cell adhesion and cell proliferation. Therefore, the concentrations of the adsorbed protein on the as-prepared HA 2D films were determined. From Figure 7(e), the concentrations of the adsorbed protein on control

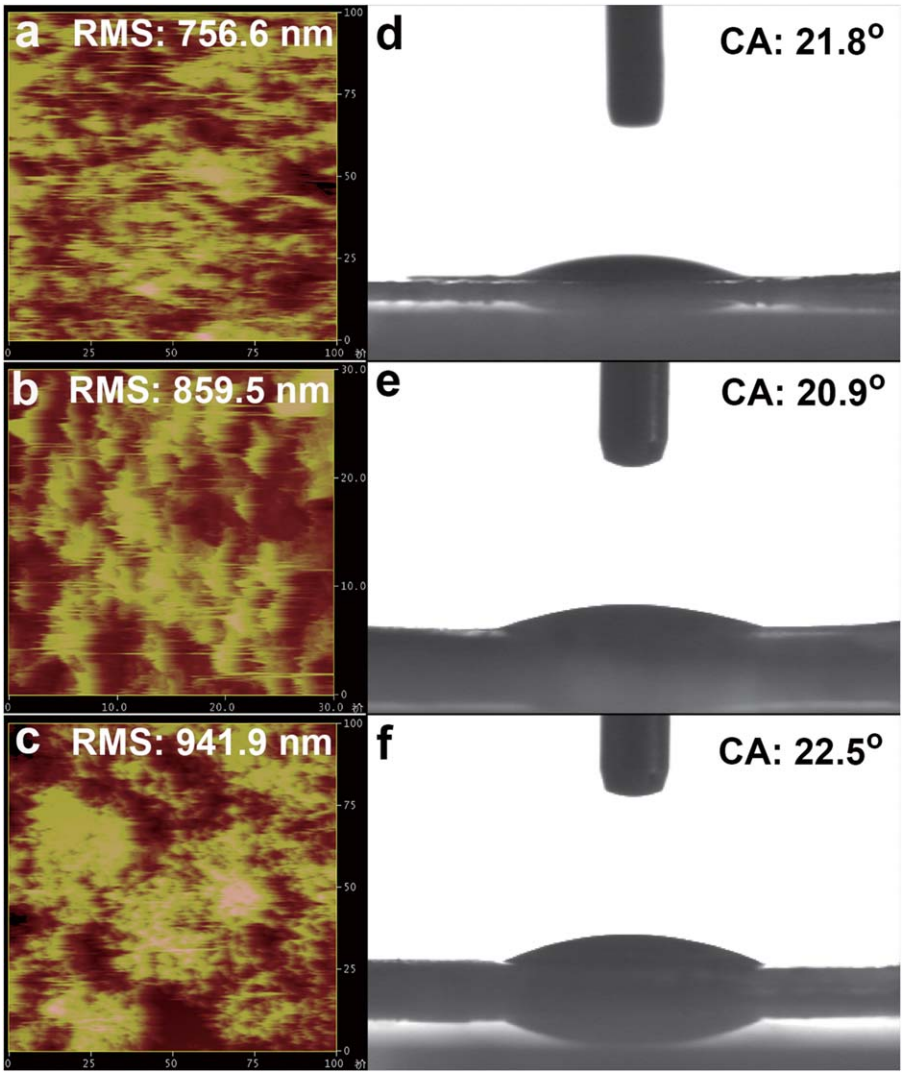

FIGURE 5. AFM images of (a) HA-Asp-PLA, (b) HA-Arg-PLA, and (c) HA-Gly-PLA 2D films. Optical images of the water contact angles measurement of (d) HA-Asp-PLA, (e) HA-Arg-PLA, and (f) HA-Gly-PLA 2D films.

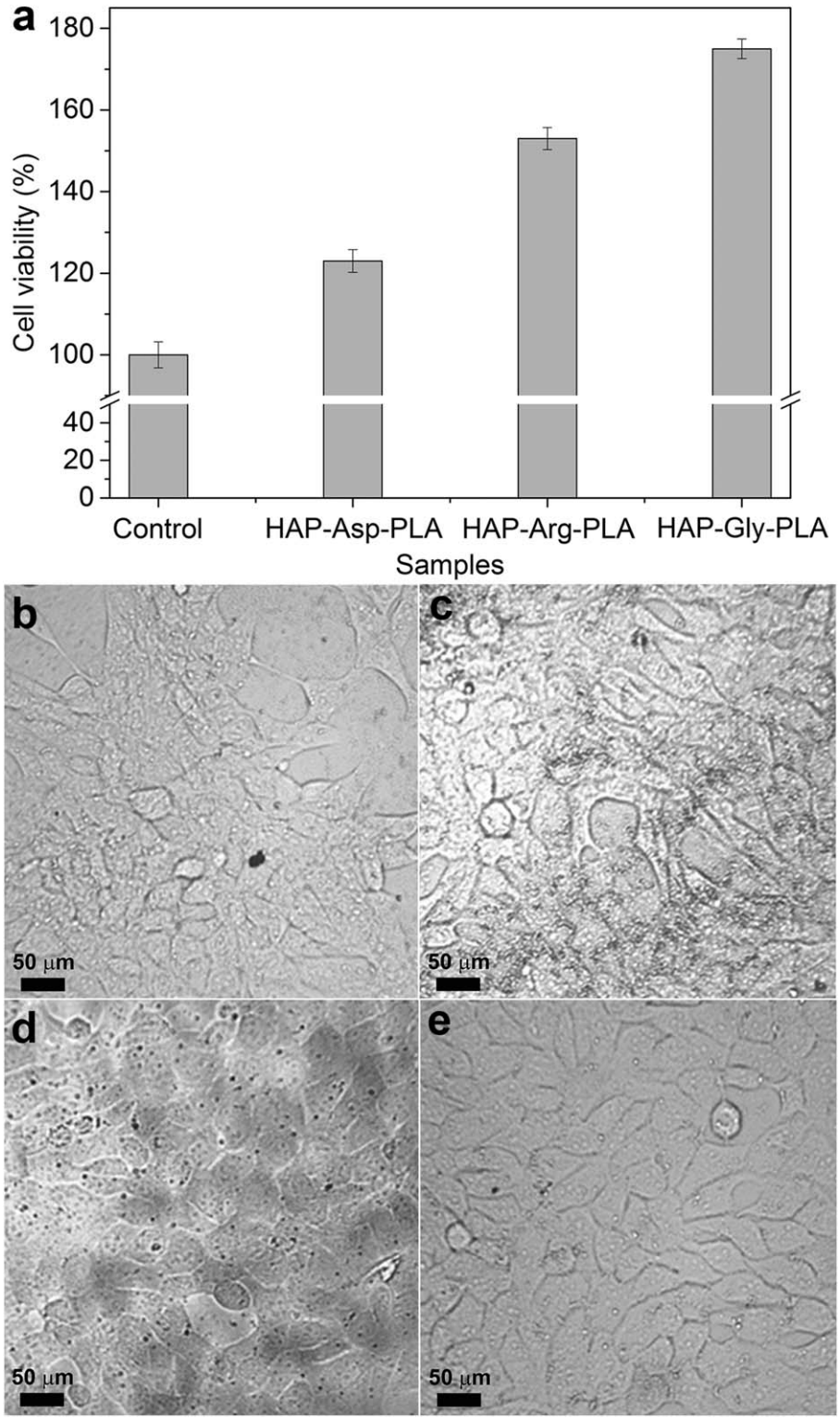

FIGURE 6. (a) The viabilities of hFOB 1.19 cells cultured on different HA 2D films. Each data point represents the mean ± S.D., $n = 3$. (b–e): Optical micrographs of hFOB 1.19 cells after cultured under different conditions for 72 h. (b) control wells without any films, (c) HA-Asp-PLA, (d) HA-Arg-PLA, and (e) HA-Gly-PLA 2D films.

wells, HA-Asp-PLA, HA-Arg-PLA, and HA-Gly-PLA 2D films are 1.68 μg/mL, 3.21 μg/mL, 3.74 μg/mL, and 4.96 μg/mL, respectively. These results indicate that the capacities of the HA 2D films to adsorb proteins from cell culture medium are considerably higher than that of the control well.

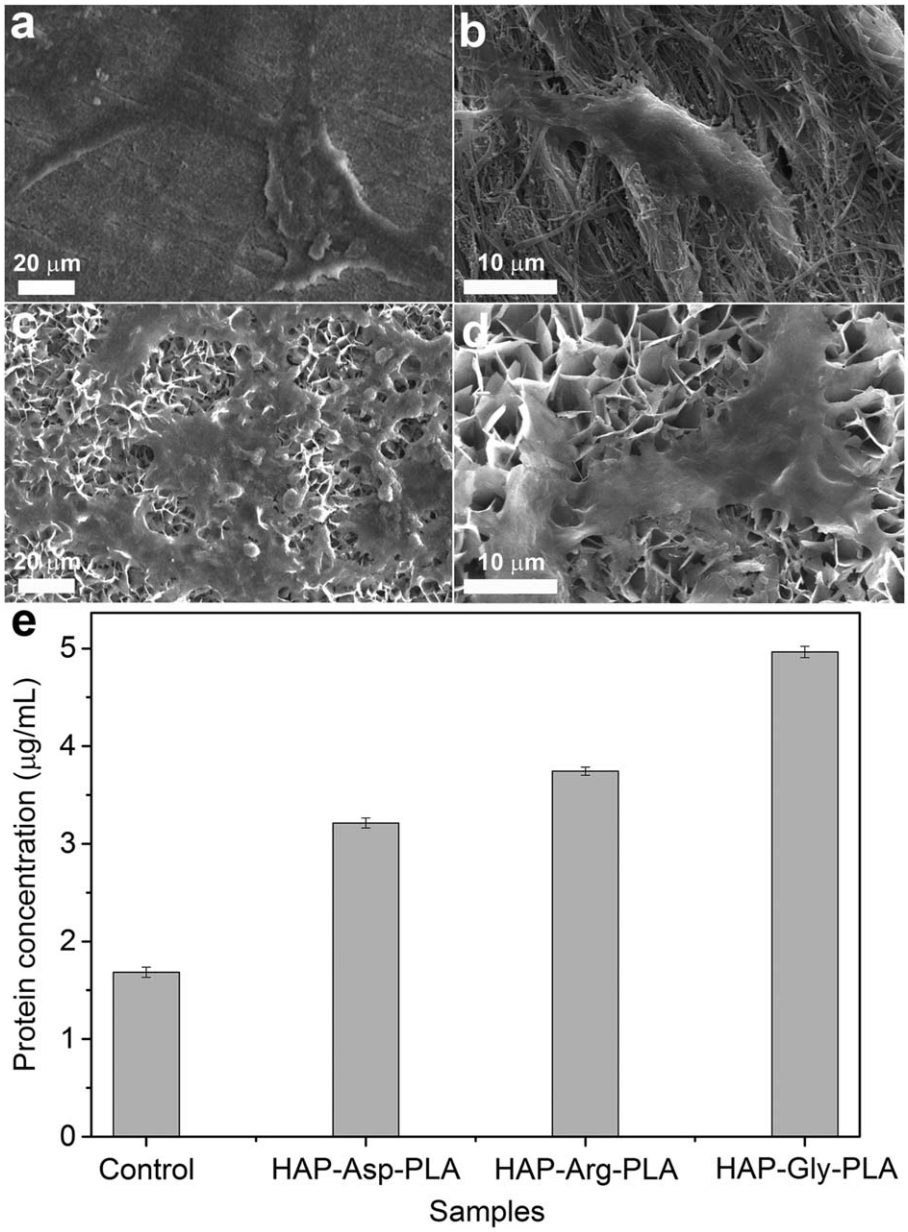

FIGURE 7. SEM images of hFOB 1.19 cells cultured under different conditions for 72 h. (a-b) control wells without any films, (c-d) HA-Arg-PLA 2D films. Protein adsorption capacities of HA 2D films determined by BCA assay. Each data point represents the mean ± S.D., $n = 3$.

DISCUSSION

In the present study, using Asp, Arg, and Gly as additives and hydrated PLA discs as substrates, three HA 2D films with different topological roughness but similar wettability can be successfully prepared through a facile one-step strategy.

The results indicate that the hydration pre-treatment can considerably enhance the roughness and wettability of the PLA discs. Furthermore, the attempt to prepare PLA 2D films on unhydrated and hydrated PLA discs reveals that HA 2D films can be successfully prepared on hydrated PLA discs. However, HA 2D films cannot be formed on unhydrated PLA discs. These demonstrate that the hydration pre-treatment of PLA discs is critical for the successful formation of HA 2D films.

From the AFM characterization results, depending on the kind of the amino acids, three different HA 2D films exhibit different topological roughness. However, the water CA evaluation results reveal that three different HA 2D films own similar wettability, independent of the kind of the amino acids. These results indicate that the topological roughness of HA 2D films prepared in this study can be easily adjusted through the careful selection of the amino acids. Moreover, the wettability of the HA 2D films is not affected by the adjustment of the topological roughness. This clearly discloses that it is possible to successful adjust the topological roughness of the inorganic 2D films on the premise of the preservation of the wettability.

From literature, Asp, Arg, and Gly own the negatively charged, positively charged, and nonpolar side chains,

respectively.[27] Therefore, these amino acids exhibit different interactions with the hydrated PLA discs, which lead to their different absorption behaviors on the surface of the discs. On absorbed onto the discs, the absorbed amino acids can interact Ca^{2+} and results in the different arrangement of Ca^{2+} on the surface of the discs. Finally, HA 2D films with different topological roughness but similar wettability are formed through the reaction of Ca^{2+} with PO_4^{3-}.

From MTT colorimetric assay results, the as-prepared HA 2D films can significantly promote the proliferation of the osteoblast cells. Furthermore, with the increase of the topological roughness of the HA 2D films, the pro-proliferation effect of the 2D films on osteoblast cells increase significantly. Considering the same chemical composition, similar wettability, and different topological roughness, this result clearly reveals that the different promotion effects of the different HA 2D films on the proliferation of osteoblast cells can be ascribed to the different topological roughness of the HA 2D films. Consequently, this hints that the pro-proliferation activity of the films can be efficiently adjusted through the control of the roughness.

SEM observations showed that the HA 2D films exhibit the excellent biocompatibility and can significantly stimulate the adhesion and spread of hFOB 1.19 cells, suggesting their potential application in bone defects repair.

More importantly, it is found that the protein adsorption capacity of the HA 2D films increase considerably with the increase of the topological roughness. With the increase of the topological roughness, the protein adsorption capabilities of the films increase significantly. This tendency is well correlated with that of the pro-proliferation activities of the films. This demonstrates that the protein adsorption capabilities of the 2D films can affect the corresponding pro-proliferation activities and the different pro-proliferation activities of the HA 2D films can be attributed to their different protein adsorption capability.

CONCLUSION

In summary, HA 2D films with different topological properties were successfully prepared through a facile one-step method. *In vitro* results indicated that HA films exhibited different pro-proliferation effects on osteoblast cells. More importantly, the different pro-proliferation effects of the films on osteoblast can be attributed to the different topological roughness and protein adsorption capability. More importantly, these results suggest that the protein adsorption capacities of the two-dimensional materials and the corresponding cellular responses can be efficiently tuned by easily adjusting their topological properties, for example, roughness. This finding affords an efficient strategy to regulate the cellular response to bioinorganic two-dimensional assemblies and significantly expanded their application potentials in tissue engineering.

REFERENCES

1. Bass JD, Grosso D, Boissiere C, Belamie E, Coradin T, Sanchez C. Stability of mesoporous oxide and mixed metal oxide materials under biologically relevant conditions. Chem Mater 2007;19:4349–4356.
2. Fielding GA, Bandyopadhyay A, Bose S. Effects of silica and zinc oxide doping on mechanical and biological properties of 3D printed tricalcium phosphate tissue engineering scaffolds. Dent Mater 2012;28:113–122.
3. Shin H, Jo S, Mikos AG. Biomimetic materials for tissue engineering. Biomaterials 2003;24:4353–4364.
4. Spoerke ED, Murray NG, Li H, Brinson LC, Dunand DC, Stupp SI. A bioactive titanium foam scaffold for bone repair. Acta Biomater 2005;1:523–533.
5. Kim S-S, Sun Park M, Jeon O, Yong Choi C, Kim B-S. Poly(lactide-co-glycolide)/hydroxyapatite composite scaffolds for bone tissue engineering. Biomaterials 2006;27:1399–1409.
6. Ramay HRR, Zhang M. Biphasic calcium phosphate nanocomposite porous scaffolds for load-bearing bone tissue engineering. Biomaterials 2004;25:5171–5180.
7. Fujihara K, Kotaki M, Ramakrishna S. Guided bone regeneration membrane made of polycaprolactone/calcium carbonate composite nano-fibers. Biomaterials 2005;26:4139–4147.
8. Petite H, Viateau V, Bensaid W, Meunier A, de Pollak C, Bourguignon M, Oudina K, Sedel L, Guillemin G. Tissue-engineered bone regeneration. Nat Biotechnol 2000;18:959–963.
9. Dolatshahi-Pirouz A, Jensen T, Kraft DC, Foss M, Kingshott P, Hansen JL, Larsen AN, Chevallier J, Besenbacher F. Fibronectin adsorption, cell adhesion, and proliferation on nanostructured tantalum surfaces. ACS Nano 2010;4:2874–2882.
10. Dou X-Q, Li P, Zhang D, Feng C-L. RGD anchored C2-benzene based PEG-like hydrogels as scaffolds for two and three dimensional cell cultures. J Mater Chem B 2013;1:3562–3568.
11. Li P, Yin Z, Dou X-Q, Zhou G, Feng C-L. Convenient three-dimensional cell culture in supermolecular hydrogels. ACS Appl Mater Interfaces 2014;6:7948–7952.
12. Liu G-F, Ji W, Wang W-L, Feng C-L. Multiresponsive hydrogel coassembled from phenylalanine and azobenzene derivatives as 3D scaffolds for photoguiding cell adhesion and release. ACS Appl Mater Interfaces 2015;7:301–307.
13. Liu G-F, Zhang D, Feng C-L. Control of three-dimensional cell adhesion by the chirality of nanofibers in hydrogels. Angew Chem Int Edit 2014;53:7789–7793.
14. Liu G-F, Zhu L-Y, Ji W, Feng C-L, Wei Z-X. Inversion of the supramolecular chirality of nanofibrous structures through co-assembly with achiral molecules. Angew Chem Int Ed 2016;55:2411–2415.
15. Wang H-J, Cao Y, Sun Y-Y, Wang K, Cao C, Yang L, Zhang Y-D, Zheng Z, Li D, Wang J-Y, and others. Is there an optimal topographical surface in nanoscale affecting protein adsorption and cell behaviors? J Nanopart Res 2011;13:4201–4210.
16. Khang D, Lu J, Yao C, Haberstroh KM, Webster TJ. The role of nanometer and sub-micron surface features on vascular and bone cell adhesion on titanium. Biomaterials 2008;29:970–983.
17. Lim JY, Shaughnessy MC, Zhou Z, Noh H, Vogler EA, Donahue HJ. Surface energy effects on osteoblast spatial growth and mineralization. Biomaterials 2008;29:1776–1784.
18. Yang SY, Kim E-S, Jeon G, Choi KY, Kim JK. Enhanced adhesion of osteoblastic cells on polystyrene films by independent control of surface topography and wettability. Mater Sci Eng C-Mater 2013;33:1689–1695.
19. Mustafa K, Odén A, Wennerberg A, Hultenby K, Arvidson K. The influence of surface topography of ceramic abutments on the attachment and proliferation of human oral fibroblasts. Biomaterials 2005;26:373–381.
20. Kumar S, Wan C, Ramaswamy G, Clemens TL, Ponnazhagan S. Mesenchymal stem cells expressing osteogenic and angiogenic factors synergistically enhance bone formation in a mouse model of segmental bone defect. Mol Ther 2010;18:1026–1034.
21. Chen X, Sun X, Yang X, Zhang L, Lin M, Yang G, Gao C, Feng Y, Yu J, Gou Z. Biomimetic preparation of trace element-codoped calcium phosphate for promoting osteoporotic bone defect repair. J Mater Chem B 2013;1:1316–1325.
22. Wang P, Zhao L, Liu J, Weir MD, Zhou X, Xu HHK. Bone tissue engineering *via* nanostructured calcium phosphate biomaterials and stem cells. Bone Res 2014;2:14017.

23. Adams BR, Mostafa A, Schwartz Z, Boyan BD. Osteoblast response to nanocrystalline calcium hydroxyapatite depends on carbonate content. J Biomed Mater Res A 2014;102:3237–3242.
24. Salinas AJ, Esbrit P, Vallet-Regi M. A tissue engineering approach based on the use of bioceramics for bone repair. Biomater Sci 2013;1:40–51.
25. Boanini E, Torricelli P, Gazzano M, Giardino R, Bigi A. Nanocomposites of hydroxyapatite with aspartic acid and glutamic acid and their interaction with osteoblast-like cells. Biomaterials 2006; 27:4428–4433.
26. Matsumoto T, Okazaki M, Inoue M, Hamada Y, Taira M, Takahashi J. Crystallinity and solubility characteristics of hydroxyapatite adsorbed amino acid. Biomaterials 2002;23:2241–2247.
27. Nelson DL, Cox MM. Amino acids, peptides, and proteins. In: Nelson DL, Cox MM, editors. Lehninger Principles of Biochemistry. New York: W.H. Freeman and Company; 2013. p 76–80.